Chemistry & Biology
Article

Real-Time Imaging of Histone H4K12–Specific Acetylation Determines the Modes of Action of Histone Deacetylase and Bromodomain Inhibitors

Tamaki Ito,[1,3] Takashi Umehara,[4] Kazuki Sasaki,[1] Yoshihiro Nakamura,[4] Norikazu Nishino,[5] Takaho Terada,[4] Mikako Shirouzu,[4] Balasundaram Padmanabhan,[4] Shigeyuki Yokoyama,[4,6] Akihiro Ito,[1,2,7,*] and Minoru Yoshida[1,2,3,7,*]
[1]Chemical Genetics Laboratory
[2]Chemical Genomics Research Group
RIKEN Advanced Science Institute, Wako, Saitama 351-0198, Japan
[3]Graduate School of Science and Engineering, Saitama University, Saitama, Saitama 338-8570, Japan
[4]RIKEN Systems and Structural Biology Center, Tsurumi, Yokohama 230-0045, Japan
[5]Graduate School of Life Science and Systems Engineering, Kyushu Institute of Technology, Kitakyushu 808-0196, Japan
[6]Department of Biophysics and Biochemistry, Graduate School of Science, University of Tokyo, Bunkyo-ku, Tokyo 113-0033, Japan
[7]Japan Science and Technology Corporation, CREST Research Project, Kawaguchi, Saitama 332-0012, Japan
*Correspondence: akihiro-i@riken.jp (A.I.), yoshidam@riken.jp (M.Y.)
DOI 10.1016/j.chembiol.2011.02.009

SUMMARY

Histone acetylation constitutes an epigenetic mark for transcriptional regulation. Here we developed a fluorescent probe to visualize acetylation of histone H4 Lys12 (H4K12) in living cells using fluorescence resonance energy transfer (FRET) and the binding of the BRD2 bromodomain to acetylated H4K12. Using this probe designated as Histac-K12, we demonstrated that histone H4K12 acetylation is retained in mitosis and that some histone deacetylase (HDAC) inhibitors continue to inhibit cellular HDAC activity even after their removal from the culture. In addition, a small molecule that interferes with ability of the bromodomain to bind to acetylated H4K12 could be assessed using Histac-K12 in cells. Thus, Histac-K12 will serve as a powerful tool not only to understand the dynamics of H4K12-specific acetylation but also to characterize small molecules that modulate the acetylation or interaction status of histones.

INTRODUCTION

Covalent modifications of core histones play an important role in modulating chromatin structure and function. In particular, histone acetylation is a well-characterized modification that is regulated by histone acetyltransferases (HATs) and histone deacetylases (HDACs) and is evolutionarily conserved from yeast to humans (Khochbin et al., 2001; Yang and Seto, 2007). Histone acetylation occurs on lysine residues in the N-terminal tails of core histones and leads to transcriptional activation by recruiting general transcriptional factors and transcriptional coactivators to the chromatinized promoter region. Moreover, recent studies suggest that site-specific histone acetylation plays a distinct role in diverse cellular functions via generating histone codes (Strahl and Allis, 2000; Turner, 2002). For example, acetylation of histone H4K16 and H3K56 is critical for the cellular DNA damage response and double-stranded break (DSB) repair. Studies have shown that deregulated H4K12 acetylation is a biomarker of age-related impairment in hippocampus-dependent memory formation in mice (Sharma et al., 2010; Peleg et al., 2010). The histone code hypothesis, initially proposed by Jenuwein and Allis (2001), suggests that various combinations of histone modifications constitute an epigenetic marking system that regulates specific and distinct functional outputs of eukaryotic genomes. These epigenetic marks are ''written'' by histone-modifying enzymes, ''read'' by proteins that specifically bind to single or combined histone modification site(s), and ''erased'' by histone demodification enzymes (Chi et al., 2010). Therefore, when, where, and how site-specific histone acetylation is induced or maintained in living cells should be tightly regulated. However, to date, there has not been a method that can be used to analyze and quantify site-specific histone acetylation levels in living cells at a high spatial and temporal resolution. Recently, we successfully developed the first fluorescent probe, named Histac, that visualizes acetylated K5/K8 of histone H4 in living cells. This technique was based on the idea that conformational changes upon acetylation can alter FRET generated in the fusion protein of histone H4 and testis-specific bromodomain-containing protein (BRDT), which was further tandemly fused with donor and acceptor fluorescent proteins (Sasaki et al., 2009). Using Histac, we demonstrated the dynamic fluctuations in the H4K5/K8 acetylation levels during mitosis.

The bromodomain consists of approximately 110 amino acids and specifically recognizes acetylated lysine residues. Conserved bromodomains are found in many chromatin-associated proteins, including HATs such as PCAF and TAF1, and the BET family of nuclear proteins, including BRD2, BRD3, BRD4, and BRDT (Zeng and Zhou, 2002). Because a variety of transcriptional regulators and chromatin-remodeling proteins contain bromodomains, they should recognize diverse acetylated histone motifs (Agalioti et al., 2002; Hassan et al., 2002; Ladurner et al., 2003; Matangkasombut and Buratowski, 2003). Indeed, the BRD2 bromodomain specifically recognizes the acetylation of

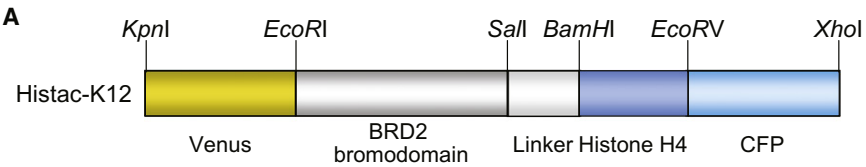

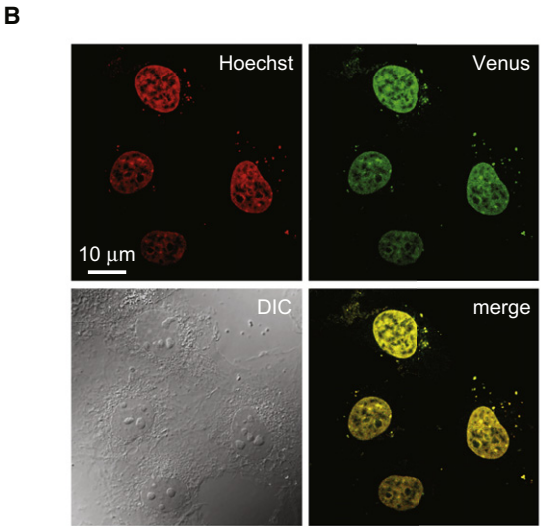

Figure 1. A Novel Fluorescent Probe for Visualizing Histone H4K12 Acetylation in Living Cells

(A) Schematic representation of the domain structure of Histac-K12.

(B) Venus and Hoechst 33342-stained images are shown in green and red, respectively. The fluorescent images were collected using a confocal microscope system.

See Figure S1.

histone H4 Lys12 (H4K12) (Kanno et al., 2004; Umehara et al., 2010a), whereas BD1 of BRDT binds to histone H4 that is diacetylated at K5 and K8 (Morinière et al., 2009). Therefore, it is possible that similar Histac-like FRET imaging probes using different bromodomains can be used to visualize different acetylation sites. In this study, we developed a novel probe that specifically recognizes H4K12 acetylation in living cells using the BRD2 bromodomain region. Using this probe, we performed a time-course analysis to demonstrate that the H4K12 acetylation level was retained during mitosis, in contrast to the decrease in H4K5/K8 acetylation in mitotic chromosomes. In addition, we analyzed the kinetics of histone acetylation upon treatment with various HDAC inhibitors. Furthermore, we showed that the probe was capable of detecting the activity of a small molecule that binds to the bromodomain cavity, which is required to recognize K12-acetylated histone H4 in living cells.

RESULTS

Design of a Novel Fluorescent Indicator to Visualize Site-Specific Acetylation

To develop a novel fluorescent probe to visualize histone H4K12 acetylation, we constructed an expression vector encoding five-part tandem fusion proteins containing the bromodomain region of BRD2, a flexible linker consisting of repeated GGGGS sequences, the substrate histone H4, and two fluorophores, CFP and Venus, which will serve as the FRET donor and acceptor, respectively (Figure 1A). We expected that the acetylation of the substrate histone H4K12 and its subsequent binding to the BRD2 bromodomain would induce a conformational change in the probe protein, thereby changing the intramolecular FRET from CFP to Venus and allowing acetylation at H4K12 to be detected. We constructed six potential indicators and evaluated their ability to change the 480 nm/535 nm emission ratio in response to trichostatin A (TSA) (Yoshida et al., 1990), a potent HDAC inhibitor, in cultured cells (see Figures S1A and S1B available online). We designated the most promising probe, VB4HC, as Histac-K12, and chose it for further study (Figure 1A; Figure S1A).

Histac-K12 colocalized with nuclear DNA that was stained with Hoechst 33342 in COS7 cells (Figure 1B). To further investigate whether Histac-K12 was incorporated into chromatin, we fractionated extracts of cells expressing Histac-K12. Immunoblot analysis of the cytoplasmic (Cy), nucleoplasmic (Nu), and chromatin (Ch) fractions showed that Histac-K12 was localized in the chromatin fraction (Figure S1C). In addition, we examined the effects of Histac-K12 expression on chromatin structure using micrococcal nuclease digestion, which can distinguish the nucleosomal formation levels from the sizes of DNA corresponding to the nucleosomal repeats. The micrococcal nuclease digestion pattern of Histac-K12–expressing COS7 cells was comparable to that of the untransfected control cells, suggesting that Histac-K12 is incorporated into chromatin without causing apparent abnormalities in the nucleosome.

Next, we verified whether the acetylation kinetics in the probe in response to TSA is similar to that in endogenous H4. The acetylation of Histac-K12 in COS7 cells could be detected within 3 hr after TSA treatment (Figure 2A). A time course showed that endogenous histone H4K12 had similar acetylation kinetics. Figure 2B and Movie S1 show images of a COS7 cell expressing Histac-K12 upon TSA treatment; the 480 nm/535 nm emission ratio is indicated with pseudocolors. The response reached a plateau within 3 hr after TSA treatment (Figure 2C). Immunoblot analysis showed that the length of time required to reach the plateau was similar to that for Histac-K12 acetylation (Figures 2A and 2C). After removing TSA from the culture, both the emission ratio and acetylation of Histac-K12 rapidly returned to basal levels, indicating that Histac-K12 is a reversible indicator of histone H4 acetylation in living cells (Figure 2E; Figure S2B and Movie S2). Photobleaching of Venus resulted in an increase in CFP fluorescence (Figure S2A), and the photobleached indicator no longer

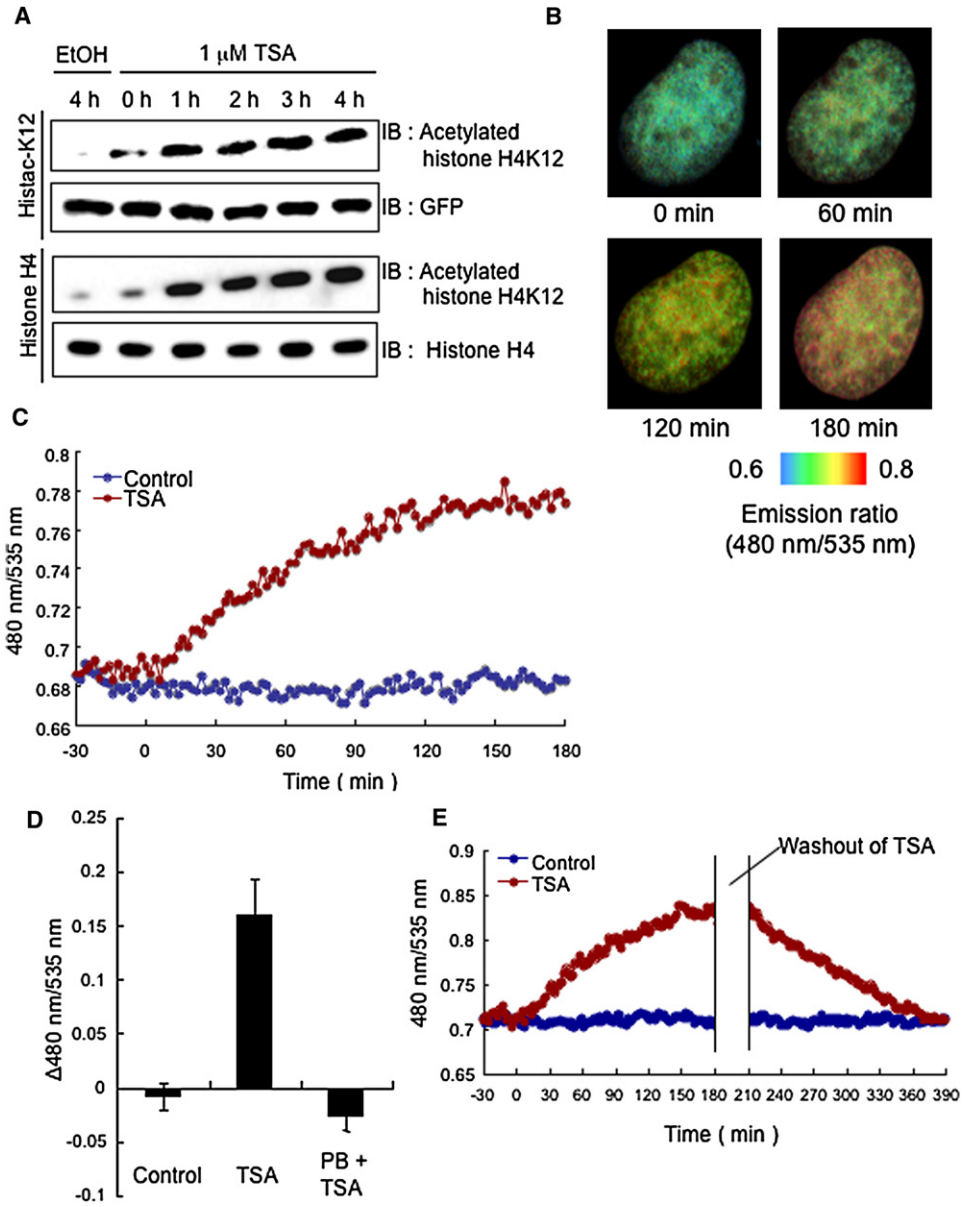

Figure 2. FRET Response of Histac-K12 to Acetylation of Histone H4K12 after TSA Stimulation

(A) Histac-K12–expressing COS7 cells and untransfected COS7 cells were treated with 1 μM TSA. Immunoblot analyses were performed using antibodies against GFP, histone H4, and histone H4 acetylated at Lys12.

(B and C) Pseudocolored images and a time course of the emission ratio in the nucleus of a Histac-K12–expressing COS7 cell. TSA at a final concentration of 1 μM or the vehicle control was added to the culture at 0 min.

(D) Changes in the emission ratio (mean ± SD) in cells that were treated with 1 μM TSA for 3 hr after Venus within Histac-K12 was photobleached. Asterisk indicates $p < 0.05$ compared with Histac-K12 and Histac-K12 treated with TSA, respectively.

(E) Emission ratio time courses of cells expressing Histac-K12 treated with TSA. TSA was added to the culture at 0 min and washout at 180 min.

See Figure S2 and Movies S1 and S2.

responded to TSA (Figure 2D), indicating that the change in the emission ratio reflects the change in FRET from CFP to Venus.

We also examined the dose response of Histac-K12 to TSA treatment. The minimum concentration of TSA required to induce a change in the emission ratio was approximately 1 nM (Figures 3A and 3B). In contrast, 10 nM of TSA was required to detect the change in acetylation by immunoblotting (Figures 3C and 3D). Thus, Histac-K12 is more sensitive than immunoblot analysis to detect histone H4K12 acetylation.

Mutational Analysis of Acetylation Sites and Acetylation-Binding Domains

To verify that the TSA-induced change in FRET reflects the acetylation of H4K12 in the probe, we tested the effects of mutating

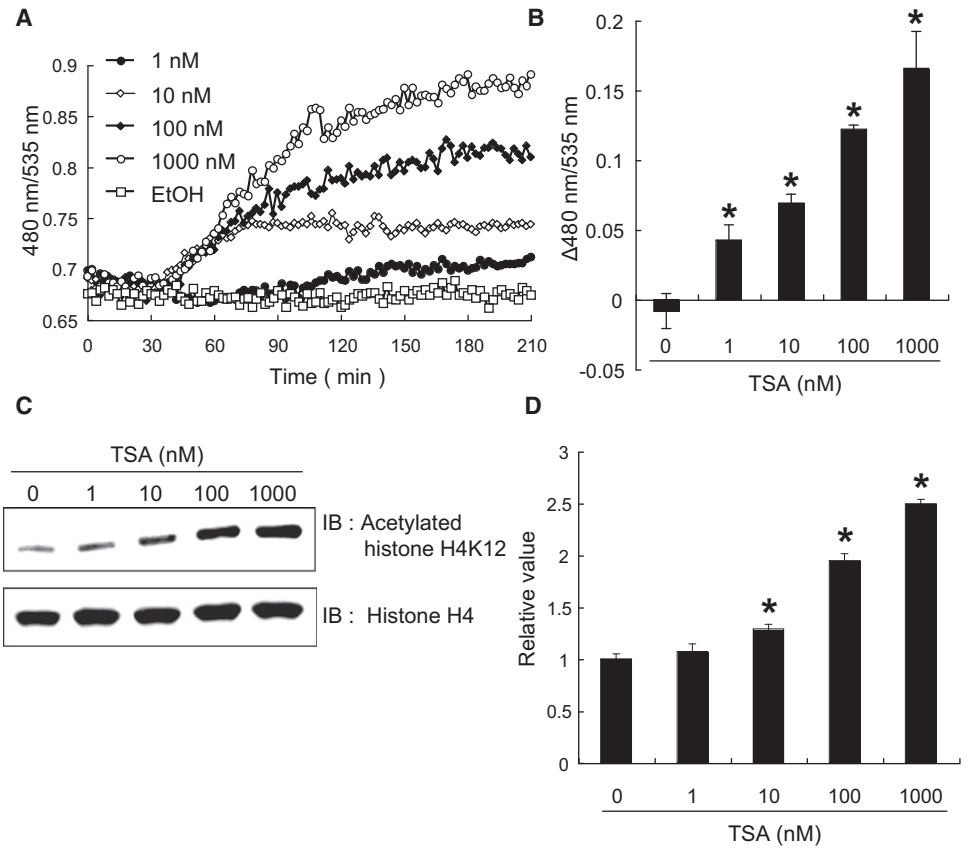

Figure 3. Comparison of Immunoblotting Analysis with Imaging Analysis Using Histac-K12

(A and B) Time course of the emission ratio (A) and changes in the emission ratios (B) of Histac-K12–expressing cells that were treated with TSA. Data are the means ± SD from three independent experiments. Asterisk indicates $p < 0.05$ compared with control.

(C and D) The immunoblot analysis was performed with antibodies against histone H4 and histone H4 acetylated at Lys12. COS7 cells were treated with various concentrations of TSA at 37°C for 3 hr. Data are the means ± SD from three independent experiments. Asterisk indicates $p < 0.05$ compared with control.

the acetylation sites in histone H4 of the probe. Substituting arginines for the lysine residues at all four acetylation sites (K5, K8, K12, and K16) of histone H4 in the probe (4KR) resulted in a loss of the response to TSA treatment (Figure 4A). Replacing K12 with arginine also dramatically decreased the response to an almost undetectable level. In clear contrast, any single substitutions at K5, K8, or K16 or the triple substitution mutant K5+8+16R did not significantly decrease the FRET response. Previous studies indicated that acetylation of histone H4K12 is one mark for newly synthesized histones (Sobel et al., 1995). Therefore, it is possible that incomplete incorporation of newly synthesized Histac-K12R resulted in the decreased response to TSA. To test this possibility, we examined whether K12R was incorporated into chromatin. Fractionation analyses showed that Histac-K12R was normally incorporated into chromatin (Figure S1C). These data demonstrate that Histac-K12 is a specific indicator that can be used to visualize the acetylation of histone H4K12.

Next we examined the effects of mutations in the Histac-K12 BRD2 bromodomain on the FRET response in order to confirm the role of the bromodomain. The bromodomain is generally composed of four α helices with two loops (Zeng and Zhou, 2002). The BRD2 bromodomain consists of two domains, BD1 and BD2. Y113 and Y386 in the loops of BD1 and BD2, respectively, are highly conserved throughout the large family of bromodomain-containing proteins, such as PCAF, GCN5, TAF1, CBP, p300 (Zeng and Zhou, 2002), and the BET family proteins (Umehara et al., 2010a; Umehara et al., 2010b). Previous studies have shown that mutating both of these tyrosine residues in the BRD2 bromodomain was sufficient to abolish the interaction with histone H4K12 (Kanno et al., 2004; Dhalluin et al., 1999; Owen et al., 2000). When these two tyrosine residues were replaced with phenylalanine (Figure 4B), the double-bromodomain mutant (BD1+2Y/F) was incapable of binding to acetylated histone H4 (Figure 4C) and failed to respond to TSA in vivo (Figure 4D). Importantly, the single Y113F mutant in BD1 (BD1Y/F) was sufficient to impair both the ability to bind to acetylated histone H4 (Figure 4C) and the FRET response to TSA treatment (Figure 4D). In contrast, the Y386F mutant in BD2 (BD2Y/F) retained the ability to bind to acetylated histone H4 (Figure 4C) and showed a similar change in the emission ratio as wild-type (WT) (Figure 4D). These data clearly indicate that BD1 plays a primary role in recognizing acetylated H4K12, which was supported by the observation that substituting alanine for Y113 (Y113A) decreases BD1 binding to the acetylated H4K12 tail peptide, as measured by surface plasmon resonance (SPR) spectroscopy (Umehara et al., 2010a).

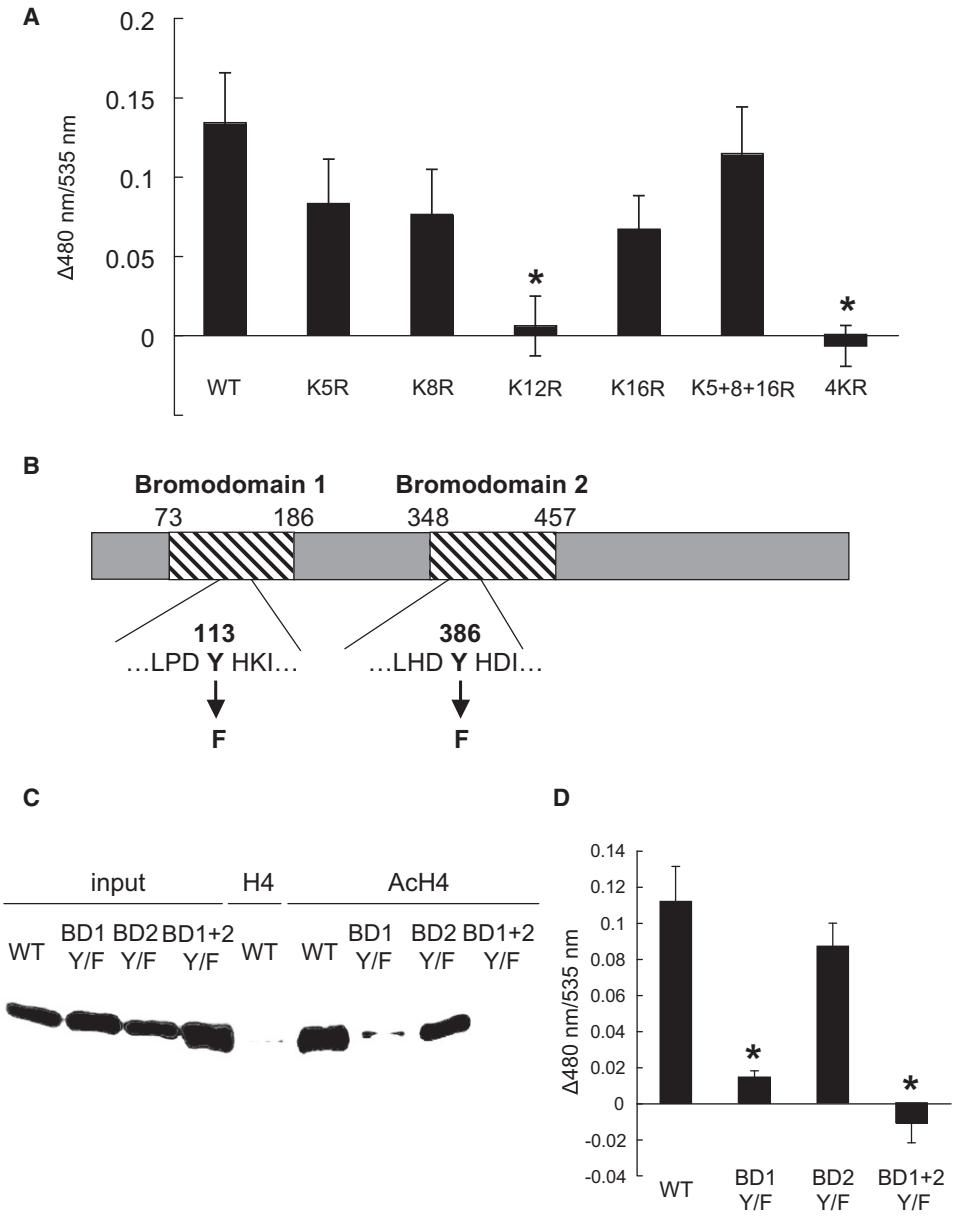

Figure 4. Mutational Analysis of Acetylation Sites and Acetylation-Binding Domains

(A) Changes in the emission ratio (mean ± SD) of Histac-K12 mutants that were exposed to 1 μM TSA for 3 hr. Asterisk indicates $p < 0.05$ compared with Histac-K12.

(B) The schematic representation shows the domain structure of BRD2. YF is a bromodomain mutant in which Tyr113 and 386 of BRD2 are replaced with Phe.

(C) Peptide pull-down assay using unmodified or acetylated (Ac) histone H4 N-terminal tail peptides. Pull-downs were analyzed by immunoblotting using an anti-GFP antibody.

(D) Changes in the emission ratio of Histac-K12 mutants that were treated with 1 μM TSA for 3 hr. Data are the means ± SD from three independent experiments. Asterisk indicates $p < 0.05$ compared with Histac-K12.

See Figure S3.

Live Imaging of Histac-K12 During Mitosis

Using Histac, we previously showed that acetylation of histone H4K5/K8 was decreased during mitosis but recovered in G1 phase (Sasaki et al., 2009). To test whether H4K12 acetylation is similarly regulated throughout the cell cycle, we monitored the H4K12 acetylation levels using Histac-K12 and found that H4K12 acetylation was maintained during mitosis (Figures 5A and 5B and Movie S3). Consistent with this finding, the levels of acetylated histone H4K12 detected by immunoblotting were retained even in M phase cells that were arrested with nocodazole, unlike the drastic decreases in the levels of acetylated histones H4K5 and K8 (Figure 5C).

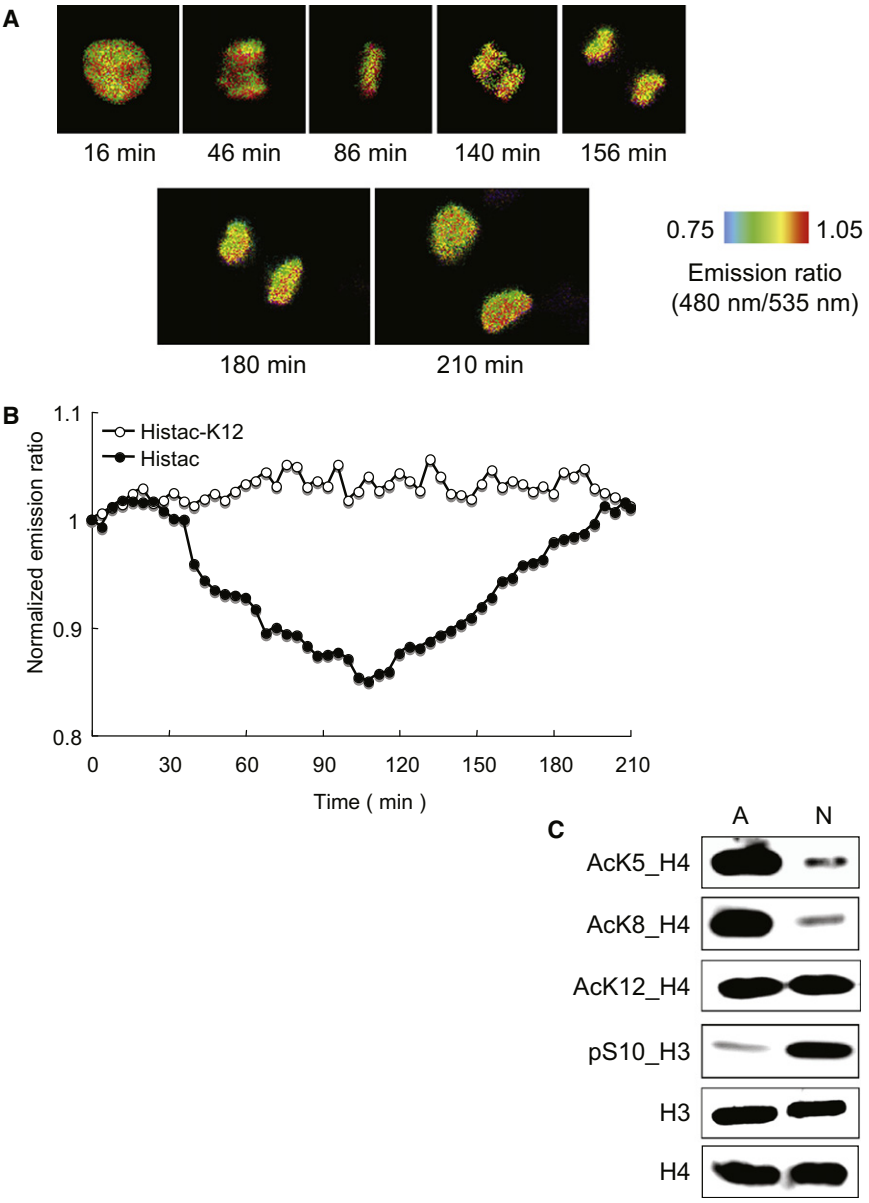

Figure 5. Live Imaging of Histac-K12 During Mitosis

(A) Pseudocolored images of the 480 nm/535 nm emission ratio obtained from a COS7 cell expressing the acetylation indicator during mitosis.

(B) Time courses of the 480 nm/535 nm emission ratio of Histac-K12 (○) and Histac (●).

(C) The acetylation of histone H4 at K12 asynchronous (A) and nocodazole-treated (N) COS7 cells was analyzed by immunoblotting using antibodies against histone H4 acetylated at K5, K8, and K12. Phosphorylated histone H3S10 (pS10), a mitotic marker, was analyzed by immunoblotting using an antibody against phosphorylated histone H3. COS7 cells were arrested in mitosis by treating with 50 ng/ml nocodazole for 8 hr.

See Movie S3.

Evaluation of HDAC Inhibitors in Living Cells

Acetylation of histone H4K12 has been associated with the general transcription of cell cycle–related genes (LeRoy et al., 2008), genetic disorders such as the neurodegenerative disease Friedreich's ataxia (Herman et al., 2006), and age-dependent memory impairment (Peleg et al., 2010). Because H4K12 acetylation is dynamically regulated throughout the genome, Histac-K12 is a suitable tool to characterize the cellular response to HDAC inhibitors. TSA is a potent pan-HDAC inhibitor that reversibly blocks the activity of essentially all class I and II HDACs. On the other hand, trapoxin B (TPX B) (Figure S4A) is another microbial metabolite that inhibits class I and II HDACs, except HDAC6 (Kijima et al., 1993; Matsuyama et al., 2002). In contrast to TSA, TPX B is a tight-binding inhibitor, likely because it covalently binds to the catalytic pocket via its epoxyketone moiety. Therefore, we tested the reversibility of enzyme inhibition by these inhibitors using Histac-K12. In contrast to the reversible response to TSA, the acetylation levels increased by TPX B remained high even after it was removed, confirming that TPX B is a tight-bind and slow off inhibitor (Figures S4B and S4C). We next tested FK228 (Figure 6A), which is a cyclic depsipeptide with an intramolecular disulfide bond (Nakajima et al., 1998). We previously demonstrated that a thiol group generated from the FK228 disulfide due to the intracellular reducing activity is responsible for interacting with the active-site zinc in the catalytic pocket of HDAC enzymes (Furumai et al., 2002). We detected a rapid increase in histone H4K12 acetylation after adding FK228 (Figure 6B). However, histone H4K12 acetylation induced by FK228 was persistent after FK228 removal from the medium; the emission ratio remained unchanged for 24 hr after FK228 was removed from the culture (Figure S4D). This long-term acetylation of endogeneous histone H4K12 and Histac-K12 was verified by immunoblot analysis (Figure 6C; Figure S4F). Because it is possible that the tight binding of the thiol group to the HDAC pocket zinc was generally responsible for the stable H4K12 acetylation, we also examined the reversibility of histone H4K12 acetylation by Ky-6 (Nishino et al., 2003) (Figure 6A), which also contains a disulfide bond. The Ky-6 activity was reversible, and both the emission ratio and the acetylation level in immunoblot analyses reverted to the original levels 2 hr after drug removal (Figures 6D and 6E). These results suggest that a structure other than the disulfide bond in FK228 is responsible for the lasting inhibition in vivo. Finally, we tested MS-275, which is a clinically studied synthetic benzamide derivative (Figure 6A) (Saito et al., 1999). MS-275–treated cells also showed a continuous response for at least 24 hr after compound removal (Figure 6F; Figure S4F), which was also confirmed by immunoblotting (Figure 6G; Figure S4G).

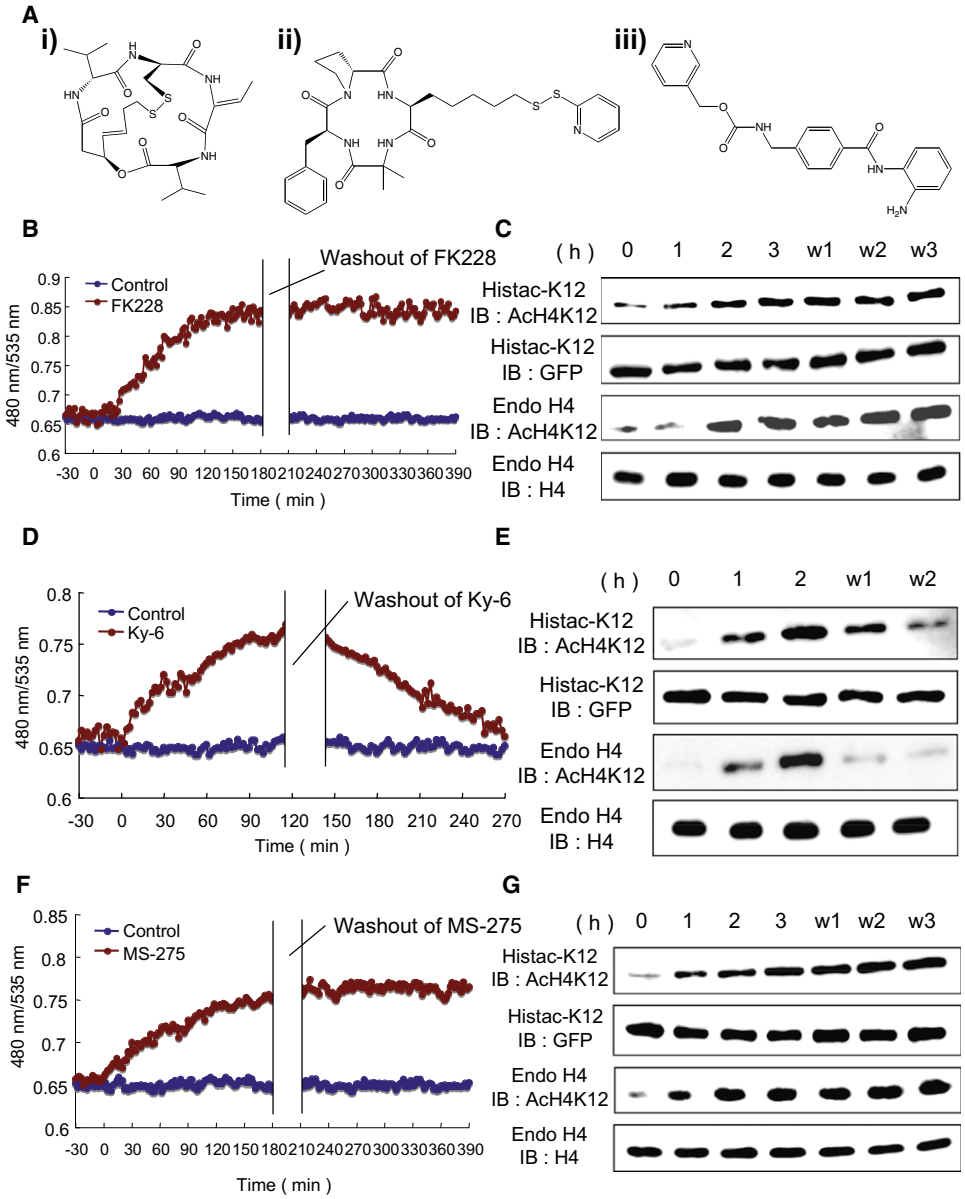

Figure 6. Dynamics Analysis of Acetylation of Histone H4K12 in Living Cells Using Various HDAC Inhibitors

(A) Structure of HDAC inhibitors FK228 (i), Ky-6 (ii), and MS-275 (iii).

(B–G) Time courses of the emission ratio (B, D, and F) and acetylation of histone H4K12 (C, E, and G) in Histac-K12-expressing cells that were treated with FK228 (B and C), Ky-6 (D and E), or MS-275 (F and G). Each HDAC inhibitor was added to the culture at 0 min and washed out at 180 min for FK228 and MS-275 or 120 min for Ky-6.

See Figure S4.

Identification and Evaluation of a Bromodomain Inhibitor Using Histac-K12

Because Histac-K12 can detect changes in the physical interaction between acetylated histone H4K12 and the BRD2 bromodomain, it is theoretically possible to detect not only HAT or HDAC inhibitors that change the acetylation status but also compounds that directly interfere with the interaction between acetylated H4K12 and the BRD2 bromodomains on the basis of changes in the emission ratio of this probe. To validate the potential usefulness of Histac-K12 to detect such a bromodomain inhibitor, we used Histac-K12 to screen for an inhibitor of BD1 in BRD2. On the basis of our crystal structures of the BRD2-BD1 bromodomain (Umehara et al., 2010a; Nakamura et al., 2007), we searched for compounds that interact with BRD2-BD1 among commercially available compounds using a combination of computational and biochemical analyses. The structural coordinates of the residues composing the BRD2-BD1 bromodomain (PDB ID: 1x0j) were used for computational docking screening,

using the Dock 4.0 and Autodock 3.0.5 programs, against a nonredundant compound library of nine compound databases. On the basis of top scores of the docking calculations, we selected 192 compounds out of 628,402 compounds that were filtered out according to Lipinski's rule of five (Lipinski et al., 2001). Then we examined the ability of each of these 192 compounds to biochemically interact with the BRD2-BD1 bromodomain by SPR and identified four candidate compounds as potential BRD2-BD1–interactive compounds (data not shown). These compounds were further screened using Histac-K12–expressing COS7 cells. When the cells were treated only with TSA, we observed a marked increase in the change of the emission ratio, as expected (Figure 7A). Interestingly, when the cells were treated with TSA and one of the four candidate compounds, which was designated BIC1 (BRD2-interactive compound-1), the increase in the emission ratio was markedly suppressed in a dose-dependent manner (Figure 7A). These results suggest that, although K12 of Histac-K12 was hyperacetylated by TSA treatment, the BRD2-BD1 domain of Histac-K12 could not bind to the H4 region, presumably because BIC1 bound to the BD1 domain of the probe and blocked its ability to bind to acetylated H4K12. Immunoblot analysis showed that BIC1 did not affect the acetylation level of Histac-K12 or that of endogeneous histone H4K12 in TSA-treated cells, indicating that BIC1 inhibited the interaction between the BRD2 bromodomain and acetylated histone H4K12 without affecting the K12 acetylation of histone H4 (Figure S5A). Of note, the increase in emission ratio of Histac in response to TSA was partially suppressed by BIC1 (Figure S5B), suggesting that BIC1 also weakly inhibits the interaction between the BRDT bromodomain and acetylated histone H4. The chemical structure of BIC1, 1-[2-(1H-benzimidazol-2-ylthio)ethyl]-1,3-dihydro-3-methyl-2H-benzimidazole-2-thione, is shown in Figure 7B. We also confirmed that BIC1 directly interacted with the BRD2-BD1 protein with a dissociation constant of 28 ± 0.2 μM, as measured by SPR spectroscopy (Figure 7C).

Inhibition of BRD2-Dependent Transcription by the BIC1 Compound

To date, the strongest binding between an acetylated histone tail and a BET bromodomain is 21.9 μM, which was observed between the K5/K8-diacetylated H4 tail and the BD1 bromodomain of BRDT (Morinière et al., 2009). The dissociation constant of the K12-acetylated H4 tail from the BRD2-BD1 protein is 930 μM (Umehara et al., 2010a). Thus, BIC1 is assumed to inhibit the BRD2 bromodomain in vivo. Because BRD2 enhances the promoter activity of mammalian cells in response to active *Ras* (*RasV12*) through the association of the bromodomains with K12-acetylated histone H4 (Kanno et al., 2004; Denis et al., 2000), we examined whether BIC1 represses the BRD2-dependent transcriptional activation of a reporter gene in HeLa cells. We established a luciferase assay system in which the *luciferase* gene driven by the SV40 promoter was activated approximately six-fold in the presence of *RasV12* when the full-length *BRD2* was introduced (Figure 7D). As expected, the addition of BIC1 at final concentrations of 5 μM or 10 μM significantly decreased the BRD2-dependent transcriptional activation of the *luciferase* gene (Figure 7D), suggesting that BIC1 is capable of blocking the transcriptional activity of BRD2 in human cells.

Crystal Structure Analysis of the BIC1-Bound BRD2 Bromodomain

To confirm that BIC1 directly binds to the bromodomain cavity of BRD2-BD1, we solved the crystal structure of the compound-bound form of BRD2-BD1. After soaking the apo-form of BRD2-BD1 crystals in a BIC1-containing solution, we obtained an F_o - F_c electron density map showing that BIC1 bound to the BRD2-BD1 cavity and solved the crystal structure of the compound-bound BRD2-BD1 domain at 2.30 Å resolution. The crystallographic statistics are summarized in Table S1.

As shown in Figure 7E, one benzimidazole ring of BIC1 is located in the BRD2-BD1 cavity, and the other benzimidazole-2-thione ring is located at the cavity periphery. In the cavity, one of the two nitrogen atoms of the benzimidazole ring forms hydrogen bonds with the carbonyl group of the P98 main chain of BRD2-BD1 and with a water molecule (Figure 7E). The direction of the aromatic benzimidazole ring seems to be hydrophobically stabilized by V103 and I162. At the periphery of the BRD2-BD1 cavity, the benzimidazole-2-thione ring hydrophobically interacts with the side chains of W97 and I162, which is different from the binding mode of the natural substrate, the K12-acetylated histone H4 tail (Figure 7F). These structural analyses revealed that BIC1 interacts with the bromodomain cavity of BRD2-BD1, indicating the mechanism by which this compound prevents BRD2 from associating with acetylated H4K12.

DISCUSSION

Technical limitations have made it extremely difficult to spatially and temporally analyze histone acetylation in vivo. We previously developed Histac, the first fluorescent probe that can specifically visualize acetylated H4K5/K8 in living cells using FRET (Sasaki et al., 2009), in which the emission ratio is altered when a conformational change is induced via the interaction between acetylated histone H4K5/K8 and the BRDT bromodomain. Indeed, HDAC inhibitors such as TSA greatly increased the emission ratio by inducing histone hyperacetylation. In this study, we used this technology to develop a novel fluorescent probe, Histac-K12, which allows histone H4K12 acetylation to be visualized in living cells. Histac-K12 was incorporated into chromatin and was acetylated with kinetics that were similar to those the acetylation of endogenous histone H4K12. The emission ratio was not increased when the probe was mutated at K12 (Histac-K12R). Therefore, the interaction between acetylated lysine and the BRD2 bromodomain seems to occur only on the same probe molecule, although the X-ray crystal structure indicates that it is possible for the bromodomain to access the acetylation site of the endogenous histone H4 molecule packed into the same nucleosome (Sasaki et al., 2009; Harp et al., 2000; Huston et al., 1988). Interestingly, immunoblot analysis showed that acetylation at K5 in Histac-K12R also decreased to an almost undetectable level (Figure S3). These results suggest that acetylation at K5 and possibly K8 is regulated by K12 acetylation, as was previously reported (Sasaki et al., 2009).

The dynamic behavior of histone H4 acetylation during mitosis remains obscure. Using Histac, we previously showed that K5/K8 acetylation is dramatically reduced in metaphase and anaphase. It is possible that histone deacetylation is involved

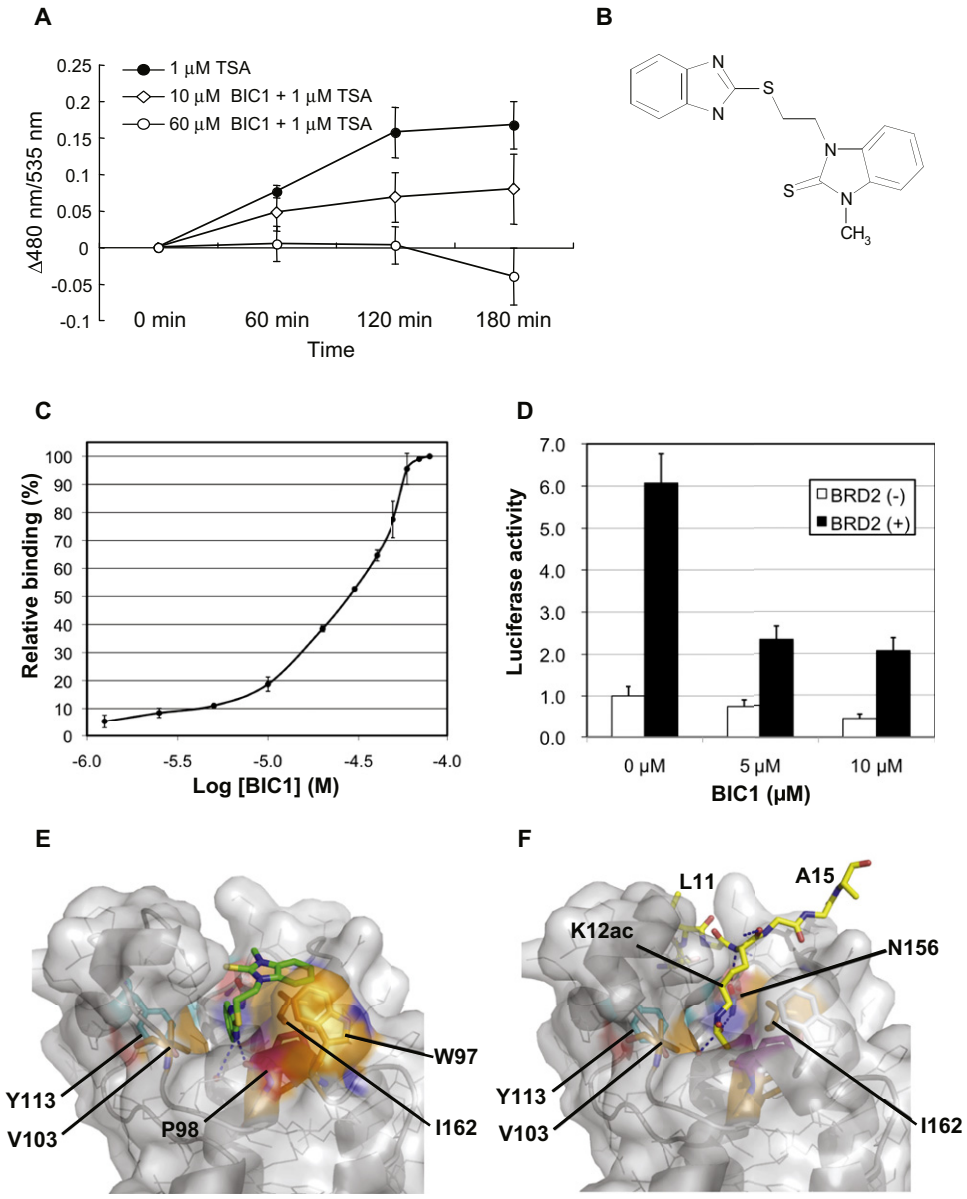

Figure 7. Identification and Evaluation of a BRD2 Bromodomain-Interactive Compound, BIC1

(A) Effects of BIC1 treatment on the Histac-K12 probe response. Cells expressing Histac-K12 were treated with 0, 10, or 60 μM BIC1 in the presence of 1 μM TSA to stimulate histone acetylation and were observed for 3 hr on an Olympus IX81 microscope. Inhibition of the interaction was monitored according to the change in the 480 nm/535 nm emission ratio (mean ± SD) of Histac-K12 every 1 hr.

(B) Chemical structure of BIC1.

(C) In vitro binding between BRD2-BD1 and BIC1. The dose-dependent binding results with compound concentrations ranging from 1.25 μM to 80 μM are shown. The effects of the buffer were subtracted from each binding result, and the resulting score was evaluated based on the average resonance unit at 80 μM of the compound as 100%.

(D) Inhibition of BRD2-dependent transcription by BIC1. Open and filled boxes indicate the levels of BRD2-independent and BRD2-dependent transcription, respectively.

(E) Crystal structure of BIC1-bound BRD2-BD1. BIC1 is shown in green sticks. Nitrogen and sulfur atoms are indicated in blue and yellow, respectively. The BRD2-BD1 bromodomain is shown in gray sticks with a semitransparent surface, and the water molecule that interacts with the BIC1 compound is shown as a small red ball. Y113 and N156 that are involved in recognizing the Nζ-acetylated H4 lysine are shown in cyan. Other BRD2-BD1 residues involved in the compound binding are highlighted in orange (W97, V103, and I162) or magenta (P98).

(F) Acetylated H4 tail-binding mode of BRD2-BD1. For comparison, the crystal structure of acetylated H4 tail peptide-bound BRD2-BD1 (PDB ID: 2dvq) is shown. The acetylated histone H4 tail peptide is shown as yellow sticks. Nitrogen and oxygen atoms are indicated in blue and red, respectively. "K12ac" denotes the Nζ-acetylated lysine at position 12 of histone H4.

See Table S1.

in the progression of mitosis because HDAC inhibitors cause G2/M cell cycle arrest and mitotic checkpoint activation (Yoshida and Beppu, 1988; Bolden et al., 2006). In contrast, recent studies using immunofluorescent staining and immunoblotting suggest that histone H4K12 acetylation is retained in mitosis (Kruhlak et al., 2001; Valls et al., 2005), whereas another analysis using mass spectrometry suggested that histone H4K12 is deacetylated during mitosis (Bonenfant et al., 2007). Here we demonstrated that H4K12 acetylation does not significantly change during mitosis in living cells. Interestingly, BRD4, another BET family protein, localizes to chromosomes during mitosis and has been implicated in holding mitotic memory (Dey et al., 2003). BRD4 may mark genes for transcriptional memory during mitosis, and this mark acts as a signal to initiate prompt transcription in daughter cells (Dey et al., 2009). BRD2 has also been shown to localize on mitotic chromosomes and to be involved in the transcription of cell cycle–related genes such as cyclin D1, suggesting that BRD2 is maintained throughout mitosis in order to ensure gene expression in the early G1 phase. It is likely that bromodomain-mediated recognition of acetylated H4 is crucial to retain BRD2 on mitotic chromosomes (Kanno et al., 2004). It is also possible that BRD2 protects acetylated H4K12 from deacetylating enzymes. However, Histac-K12 was a sensitive sensor that dynamically monitored not only increases but also decreases in the cellular level of H4K12 acetylation after TSA removal, suggesting that at least the BRD2 bromodomain itself within the probe cannot protect the acetylated residue from HDACs.

When evaluating various HDAC inhibitors using Histac-K12, we found that the effects of FK228 and MS-275 were long lasting in cells, whereas that of Ky-6 was rapidly reversed after removal. The action of MS-275, a synthetic benzamide derivative, requires its S3′-amino group to bind and inhibit class I HDACs (Saito et al., 1999). Importantly, the recent computational simulation suggests that benzamide derivatives form a stable complex with the active site of HDAC2 (Bressi et al., 2010), which may be responsible for the long lasting effect of MS-275 in cells. MS-275 is currently being evaluated in clinical trials as an antitumor drug (Park et al., 2004; Kazantsev and Thompson, 2008), and the clinical pharmacokinetics show that it has a long terminal half-life of 45–100 hr (Hess-Stumpp et al., 2007). The stable binding to HDAC in cells may explain its long-term effects in vivo. FK228 has an intramolecular disulfide bond and is activated in cells by reduction, which generates two thiol groups, one of which can interact with the HDAC active site (Furumai et al., 2002). Previous studies showed that FK228 can reversibly interact with the HDAC active site, as demonstrated by in vitro HDAC activity assays (Furumai et al., 2002). However, the present results are consistent with a recent study that FK228-treated cells maintained high histone acetylation levels even after the compound removal (Crabb et al., 2008). Given the reversible effect of Ky-6, another thiol-containing inhibitor, the cyclic depsipeptide structure of FK228 may be responsible for the long-lasting effect. It seems possible that an unsaturated amino acid in the depsipeptide ring forms a covalent bond with the enzyme by a Michael-type addition. The long-lasting effect of FK228 might be due to its poor efflux from cells. It is also possible that, like MS-275, the FK228-enzyme complex is stable in cells. In addition, turnover of FK228-senstive HDACs may also affect the Histac-K12 response after drug removal. Further study is needed for elucidating the mechanism of the long lasting effect of FK228.

The Histac-K12 probe was useful not only to validate H4K12 acetylation and deacetylation by several HDAC inhibitors but also to validate compounds that modulate the interaction between acetylated H4K12 and the BRD2 bromodomain. We identified BIC1 as a small molecule that inhibits the ability of the BRD2 bromodomain to bind to acetylated H4K12 (Figures 7A and 7B). BRD2 has been shown to interact with the chromatin-binding domain of latency-associated nuclear antigen 1 (LANA-1) in Kaposi's sarcoma–associated herpesvirus (KSHV). LANA-1 mediates the episomal replication of the KSHV genome and regulates transcription in latently infected cells. LANA-1 must interact with cellular chromatin for both of these functions, and BRD2 is necessary for the interaction between LANA-1 and chromatin (Viejo-Borbolla et al., 2005; Ottinger et al., 2006). Therefore, BRD2 is a promising target to prevent KSVH transmission. However, there has been no rapid and convenient method to evaluate the interaction between BRD2 and acetylated histone H4 in living cells. Using Histac-K12, we characterized the ability of BIC1 to inhibit BRD2 bromodomain binding to acetylated histone H4 in cells by monitoring the response of Histac-K12 to increased histone H4 acetylation in the presence of BIC1. We also confirmed that BIC1 bound to the BRD2-BD1 bromodomain cavity in vitro (Figure 7E) and inhibited BRD2-dependent transcription in cells (Figure 7D). Thus, Histac-K12 not only provides a novel tool to spatially and temporally analyze histone acetylation in various cellular systems, but also serves as a powerful tool to evaluate small molecules that regulate the writing, reading, and erasing of the histone H4K12 code.

SIGNIFICANCE

Site-specific histone acetylation plays an important role as an epigenetic mark, which functions as cellular memory during the cell cycle by regulating gene expression. Recently, taking advantage of specific binding of a bromodomain to acetylated lysine residues of histone H4, we succeeded in developing the first FRET-based probe for visualizing acetylated K5/K8 of histone H4 in living cells, named "Histac." To understand the dynamics of site-specific acetylation in more detail, we expanded this method to K12 of histone H4. By utilizing the bromodomain region of BRD2, which specifically recognizes K12-acetylated histone H4, we developed a probe for visualizing acetylation of histone H4K12, named Histac-K12. Using Histac-K12, we demonstrated that H4K12 acetylation is retained during mitosis in living cells. Histac-K12 allows quantitative evaluation and functional discrimination of compounds that affect H4K12 acetylation in vivo, as exemplified with three HDAC inhibitors: FK228, MS-275, and Ky-6. In addition to HDAC inhibitors, the Histac-K12 probe was also demonstrated to be useful in validating a compound that modulates the interaction between acetylated H4K12 and BRD2 bromodomain. Using Histac-K12, we identified an inhibitor for BRD2 bromodomain binding to acetylated H4K12 (BIC1) by monitoring the FRET emission ratio in the treated cells. Thus, Histac-K12 provides a novel tool not only for spatial and

temporal analysis of the H4K12 acetylation level in various cellular systems but also for evaluating regulatory factors, including small compounds that modulate acetylation of histone H4K12. Recently, Filippakopoulos et al., (2010) identified a first inhibitor of bromodomains and demonstrated the importance of the bromodomains as a target for an anticancer drug discovery. Development of novel tools such as Histac-K12 will be increasingly important for evaluating the activity of epigenetic readers.

EXPERIMENTAL PROCEDURES

Cell Imaging

After transfection, the culture medium was replaced with phenol red-free growth medium for imaging. The cells were examined at 37°C in 5% CO_2 using an Olympus IX81 microscope with a UIC-QE cooled charged-coupled device camera (Molecular Devices). Images were collected using a MetaFluor (Universal Imaging) with a 440AF21 excitation filter, a 455DRLP dichroic mirror, and two emission filters (480AF30 for CFP and 535AF26 for Venus). For Figure S2A, the images of Hoechst 33342 staining and Venus were collected with an FV1000 (Olympus) confocal microscope system.

Gel Electrophoresis and Immunoblot Analysis

For Figure 4C, the peptide pull-down assays were performed as described by Pivot-Pajot et al. (2003). COS7 cells were transiently transfected with monomeric Venus-BRD2 or the monomeric Venus-BRD2 mutants. For Figure S1C, mononucleosome core particles were purified as described by Kanda et al. (1998). The fractions were immunoprecipitated using an anti-GFP antibody (Takara Bio). The proteins were separated by SDS-PAGE and transferred to a PVDF membrane (Millipore) by electroblotting. After the membranes were incubated with the appropriate primary and secondary antibodies, the immune complexes were detected with an Immobilon Western kit (Millipore) or ECL Western Blotting Detection Reagents (GE Healthcare Bio-Science Corp.), and luminescence was analyzed with a LAS3000 mini image analyzer (Fujifilm). The antibodies that recognize acetyl-lysine 5, 8, and 12 of histone H4 and phospho-serine 10 of histone H3 were obtained from Upstate Biotechnology. The anti-histone H3, anti-histone H4, anti-GFP, and anti-FLAG antibodies were purchased from Cell Signaling Technology, Abcam, Takara Bio, and Sigma, respectively. The anti-HDAC1 and anti-tubulin antibodies were obtained from Sigma.

Surface Plasmon Resonance Analysis

To measure the dissociation constants between BRD2-BD1 and the BIC1 compound, tag-cleaved BRD2-BD1 protein was immobilized on the CM5 sensor chip (GE Healthcare) by the amine-coupling method, and SPR analysis was performed using a Biacore 3000 (GE Healthcare). The BIC1 compound (concentrations, 1.25–80 μM) was loaded for 60 s with a 10 μl/min flow rate onto the chip at room temperature, and the flow was further continued for 180 s to detect the dissociation of the proteins from the immobilized peptides in HBS-EP running buffer (10 mM HEPES [pH 7.4], 150 mM NaCl, 3 mM EDTA, and 0.005% Tween-20). Control surfaces with no protein attached were used to correct for the refractive index differences between the samples and the running buffer. The results were analyzed using the BIAevaluation software version 4.1 (GE Healthcare).

Crystal Structure Analysis

Crystallization was performed using the hanging-drop vapor-diffusion method by mixing 1.0 μl of protein solution (5 mg/ml in 20 mM Tris-HCl buffer [pH 8.0] containing 150 mM NaCl and 2 mM DTT) with 1.0 μl of various reservoir solutions, and equilibrating the mixtures against 500 ml of the reservoir solution at 20°C (Umehara et al., 2010a). Single BRD2-BD1 crystals grew within one week in a drop containing 25%–30% PEG MME 5000, 0.2 M ammonium sulfate, and 0.1 M HEPES buffer (pH 7.5). The crystals were soaked in the reservoir solution containing 5 mM BIC1 for 10–20 min and were transferred in a cryoprotectant containing 10% (w/v) glycerol. The compound-soaked crystals were flash-cooled in liquid nitrogen prior to data collection. Diffraction data were collected under cryogenic conditions using a Rigaku FR-E Cu *K*a rotating-anode X-ray generator operated at 45 kV and 45 mA and equipped with a Rigaku RAXIS IV^{2+} Imaging plate area detector and X-streamlow temperature system. The dataset was processed and scaled with the HKL2000 program suite (Otwinowski and Minor, 1997). The compound-bound structure was solved by the molecular replacement method, employing the apo-form of BRD2-BD1 as a search model (Nakamura et al., 2007). The stereochemistry of the structure is excellent, as assessed by PROCHECK (Laskowski et al., 1993). The crystallographic statistics are summarized in Table S1.

ACCESSION NUMBERS

The structural coordinates of the BRD2-BD1 bromodomain complexed with the compound BIC1 have been deposited in the Protein Data Bank under the accession code 3aqa.

SUPPLEMENTAL INFORMATION

Supplemental Information includes five figures, one table, three movies, and Supplemental Experimental Procedures and can be found with this article online at doi:10.1016/j.chembiol.2011.02.009.

ACKNOWLEDGMENTS

We thank Drs. K. Ozato (National Institute of Child Health & Human Development, National Institutes of Health) for the BRD2 plasmid; T. Takagi for the RasV12 plasmid; K. Satou, H. Hirota, and A. Tanaka for initial compound screening; E. Adachi for transfection assays; and M. Wakamori and S. Morita for protein preparation. This work was supported by RIKEN BSI's Research Resources Center for peptide synthesis, the RIKEN BSI-Olympus Collaboration Center (imaging equipment and software), the Program for Promotion of Fundamental Studies in Health Sciences of the National Institute of Biomedical Innovation (support to T.U.), the RIKEN Structural Genomics/Proteomics Initiative, the National Project on Protein Structural and Functional Analyses of MEXT (support to S.Y.), and the Targeted Proteins Research Program of MEXT (support to S.Y.).

Received: November 12, 2010
Revised: January 13, 2011
Accepted: February 1, 2011
Published: April 21, 2011

REFERENCES

Agalioti, T., Chen, G., and Thanos, D. (2002). Deciphering the transcriptional histone acetylation code for a human gene. Cell *111*, 381–392.

Bolden, J.E., Peart, M.J., and Johnstone, R.W. (2006). Anticancer activities of histone deacetylase inhibitors. Nat. Rev. Drug Discov. *5*, 769–784.

Bonenfant, D., Towbin, H., Coulot, M., Schindler, P., Mueller, D.R., and van Oostrum, J. (2007). Analysis of dynamic changes in post-translational modifications of human histones during cell cycle by mass spectrometry. Mol. Cell. Proteomics *6*, 1917–1932.

Bressi, J.C., Jennings, A.J., Skene, R., Wu, Y., Melkus, R., De Jong, R., O'Connell, S., Grimshaw, C.E., Navre, M., and Gangloff, A.R. (2010). Exploration of the HDAC2 foot pocket: synthesis and SAR of substituted N-(2-aminophenyl)benzamides. Bioorg. Med. Chem. Lett. *20*, 3142–3145.

Chi, P., Allis, C.D., and Wang, G.G. (2010). Covalent histone modifications—miswritten, misinterpreted and mis-erased in human cancers. Nat. Rev. Cancer *10*, 457–469.

Crabb, S.J., Howell, M., Rogers, H., Ishfaq, M., Yurek-George, A., Carey, K., Pickering, B.M., East, P., Mitter, R., Maeda, S., et al. (2008). Characterisation of the in vitro activity of the depsipeptide histone deacetylase inhibitor spiruchostatin A. Biochem. Pharmacol. *76*, 463–475.

Denis, G.V., Vaziri, C., Guo, N., and Faller, D.V. (2000). RING3 kinase transactivates promoters of cell cycle regulatory genes through E2F. Cell Growth Differ. *11*, 417–424.

Dey, A., Chitsaz, F., Abbasi, A., Misteli, T., and Ozato, K. (2003). The double bromodomain protein Brd4 binds to acetylated chromatin during interphase and mitosis. Proc. Natl. Acad. Sci. USA *100*, 8758–8763.

Dey, A., Nishiyama, A., Karpova, T., McNally, J., and Ozato, K. (2009). Brd4 marks select genes on mitotic chromatin and directs postmitotic transcription. Mol. Biol. Cell *20*, 4899–4909.

Dhalluin, C., Carlson, J.E., Zeng, L., He, C., Aggarwal, A.K., and Zhou, M.M. (1999). Structure and ligand of a histone acetyltransferase bromodomain. Nature *399*, 491–496.

Filippakopoulos, P., Qi, J., Picaud, S., Shen, Y., Smith, W.B., Fedorov, O., Morse, E.M., Keates, T., Hickman, T.T., Felletar, I., et al. (2010). Selective inhibition of BET bromodomains. Nature *468*, 1067–1073.

Furumai, R., Matsuyama, A., Kobashi, N., Lee, K.H., Nishiyama, M., Nakajima, H., Tanaka, A., Komatsu, Y., Nishino, N., Yoshida, M., et al. (2002). FK228 (depsipeptide) as a natural prodrug that inhibits class I histone deacetylases. Cancer Res. *62*, 4916–4921.

Harp, J.M., Hanson, B.L., Timm, D.E., and Bunick, G.J. (2000). Asymmetries in the nucleosome core particle at 2.5 Å resolution. Acta Crystallogr. D Biol. Crystallogr. *56*, 1513–1534.

Hassan, A.H., Prochasson, P., Neely, K.E., Galasinski, S.C., Chandy, M., Carrozza, M.J., and Workman, J.L. (2002). Function and selectivity of bromodomains in anchoring chromatin-modifying complexes to promoter nucleosomes. Cell *111*, 369–379.

Herman, D., Jenssen, K., Burnett, R., Soragni, E., Perlman, S.L., and Gottesfeld, J.M. (2006). Histone deacetylase inhibitors reverse gene silencing in Friedreich's ataxia. Nat. Chem. Biol. *2*, 551–558.

Hess-Stumpp, H., Bracker, T.U., Henderson, D., and Politz, O. (2007). MS-275, a potent orally available inhibitor of histone deacetylases—the development of an anticancer agent. Int. J. Biochem. Cell Biol. *39*, 1388–1405.

Huston, J.S., Levinson, D., Mudgett-Hunter, M., Tai, M.S., Novotný, J., Margolies, M.N., Ridge, R.J., Bruccoleri, R.E., Haber, E., Crea, R., et al. (1988). Protein engineering of antibody binding sites: recovery of specific activity in an anti-digoxin single-chain Fv analogue produced in *Escherichia coli*. Proc. Natl. Acad. Sci. USA *85*, 5879–5883.

Jenuwein, T., and Allis, C.D. (2001). Translating the histone code. Science *293*, 1074–1080.

Kanda, T., Sullivan, K.F., and Wahl, G.M. (1998). Histone-GFP fusion protein enables sensitive analysis of chromosome dynamics in living mammalian cells. Curr. Biol. *8*, 377–385.

Kanno, T., Kanno, Y., Siegel, R.M., Jang, M.K., Lenardo, M.J., and Ozato, K. (2004). Selective recognition of acetylated histones by bromodomain proteins visualized in living cells. Mol. Cell *13*, 33–43.

Kazantsev, A.G., and Thompson, L.M. (2008). Therapeutic application of histone deacetylase inhibitors for central nervous system disorders. Nat. Rev. Drug Discov. *7*, 854–868.

Khochbin, S., Verdel, A., Lemercier, C., and Seigneurin-Berny, D. (2001). Functional significance of histone deacetylase diversity. Curr. Opin. Genet. Dev. *11*, 162–166.

Kijima, M., Yoshida, M., Sugita, K., Horinouchi, S., and Beppu, T. (1993). Trapoxin, an antitumor cyclic tetrapeptide, is an irreversible inhibitor of mammalian histone deacetylase. J. Biol. Chem. *268*, 22429–22435.

Kruhlak, M.J., Hendzel, M.J., Fischle, W., Bertos, N.R., Hameed, S., Yang, X.J., Verdin, E., and Bazett-Jones, D.P. (2001). Regulation of global acetylation in mitosis through loss of histone acetyltransferases and deacetylases from chromatin. J. Biol. Chem. *276*, 38307–38319.

Ladurner, A.G., Inouye, C., Jain, R., and Tjian, R. (2003). Bromodomains mediate an acetyl-histone encoded antisilencing function at heterochromatin boundaries. Mol. Cell *11*, 365–376.

Laskowski, R., MacArthur, M.W., Moss, D.S., and Thornton, J.M. (1993). PROCHECK: a program to check the stereochemical quality of protein structures. J. Appl. Cryst. *26*, 283–291.

LeRoy, G., Rickards, B., and Flint, S.J. (2008). The double bromodomain proteins Brd2 and Brd3 couple histone acetylation to transcription. Mol. Cell *30*, 51–60.

Lipinski, C.A., Lombardo, F., Dominy, B.W., and Feeney, P.J. (2001). Experimental and computational approaches to estimate solubility and permeability in drug discovery and development settings. Adv. Drug Deliv. Rev. *46*, 3–26.

Matangkasombut, O., and Buratowski, S. (2003). Different sensitivities of bromodomain factorS2 and 2 to histone H4 acetylation. Mol. Cell *11*, 353–363.

Matsuyama, A., Shimazu, T., Sumida, Y., Saito, A., Yoshimatsu, Y., Seigneurin-Berny, D., Osada, H., Komatsu, Y., Nishino, N., Khochbin, S., et al. (2002). In vivo destabilization of dynamic microtubules by HDAC6-mediated deacetylation. EMBO J. *21*, 6820–6831.

Morinière, J., Rousseaux, S., Steuerwald, U., Soler-López, M., Curtet, S., Vitte, A.L., Govin, J., Gaucher, J., Sadoul, K., Hart, D.J., et al. (2009). Cooperative binding of two acetylation marks on a histone tail by a single bromodomain. Nature *461*, 664–668.

Nakajima, H., Kim, Y.B., Terano, H., Yoshida, M., and Horinouchi, S. (1998). FR901228, a potent antitumor antibiotic, is a novel histone deacetylase inhibitor. Exp. Cell Res. *241*, 126–133.

Nakamura, Y., Umehara, T., Nakano, K., Jang, M.K., Shirouzu, M., Morita, S., Uda-Tochio, H., Hamana, H., Terada, T., Adachi, N., et al. (2007). Crystal structure of the human BRD2 bromodomain: insights into dimerization and recognition of acetylated histone H4. J. Biol. Chem. *282*, 4193–4201.

Nishino, N., Jose, B., Okamura, S., Ebisusaki, S., Kato, T., Sumida, Y., and Yoshida, M. (2003). Cyclic tetrapeptides bearing a sulfhydryl group potently inhibit histone deacetylases. Org. Lett. *5*, 5079–5082.

Ottinger, M., Christalla, T., Nathan, K., Brinkmann, M.M., Viejo-Borbolla, A., and Schulz, T.F. (2006). Kaposi's sarcoma-associated herpesvirus LANA-1 interacts with the short variant of BRD4 and releases cells from a BRD4- and BRD2/RING3-induced G1 cell cycle arrest. J. Virol. *80*, 10772–10786.

Otwinowski, Z., and Minor, W. (1997). Processing of X-ray diffraction data collected in oscillation mode. Methods Enzymol. *276*, 307–326.

Owen, D.J., Ornaghi, P., Yang, J.C., Lowe, N., Evans, P.R., Ballario, P., Neuhaus, D., Filetici, P., and Travers, A.A. (2000). The structural basis of the recognition of acetylated histone H4 by the bromodomain of histone acetyltransferase Gcn5p. EMBO J. *19*, 6141–6149.

Park, J.H., Jung, Y., Kim, T.Y., Kim, S.G., Jong, H.S., Lee, J.W., Kim, D.K., Lee, J.S., Kim, N.K., Kim, T.Y., et al. (2004). Class I histone deacetylase-selective novel synthetic inhibitors potently inhibit human tumor proliferation. Clin. Cancer Res. *10*, 5271–5281.

Peleg, S., Sananbenesi, F., Zovoilis, A., Burkhardt, S., Bahari-Javan, S., Agis-Balboa, R.C., Cota, P., Wittnam, J.L., Gogol-Doering, A., Opitz, L., et al. (2010). Altered histone acetylation is associated with age-dependent memory impairment in mice. Science *328*, 753–756.

Pivot-Pajot, C., Caron, C., Govin, J., Vion, A., Rousseaux, S., and Khochbin, S. (2003). Acetylation-dependent chromatin reorganization by BRDT, a testis-specific bromodomain-containing protein. Mol. Cell. Biol. *23*, 5354–5365.

Saito, A., Yamashita, T., Mariko, Y., Nosaka, Y., Tsuchiya, K., Ando, T., Suzuki, T., Tsuruo, T., and Nakanishi, O. (1999). A synthetic inhibitor of histone deacetylase, MS-27-275, with marked in vivo antitumor activity against human tumors. Proc. Natl. Acad. Sci. USA *96*, 4592–4597.

Sasaki, K., Ito, T., Nishino, N., Khochbin, S., and Yoshida, M. (2009). Real-time imaging of histone H4 hyperacetylation in living cells. Proc. Natl. Acad. Sci. USA *106*, 16257–16262.

Sharma, G.G., So, S., Gupta, A., Kumar, R., Cayrou, C., Avvakumov, N., Bhadra, U., Pandita, R.K., Porteus, M.H., Chen, D.J., et al. (2010). MOF and histone acetylation at lysine 16 are critical for DNA damage response and double-strand break repair. Mol. Cell. Biol. *30*, 3582–3595.

Sobel, R.E., Cook, R.G., Perry, C.A., Annunziato, A.T., and Allis, C.D. (1995). Conservation of deposition-related acetylation sites in newly synthesized histones H3 and H4. Proc. Natl. Acad. Sci. USA *92*, 1237–1241.

Strahl, B.D., and Allis, C.D. (2000). The language of covalent histone modifications. Nature *403*, 41–45.

Turner, B.M. (2002). Cellular memory and the histone code. Cell *111*, 285–291.

Umehara, T., Nakamura, Y., Jang, M.K., Nakano, K., Tanaka, A., Ozato, K., Padmanabhan, B., and Yokoyama, S. (2010a). Structural basis for acetylated histone H4 recognition by the human BRD2 bromodomain. J. Biol. Chem. *285*, 7610–7618.

Umehara, T., Nakamura, Y., Wakamori, M., Ozato, K., Yokoyama, S., and Padmanabhan, B. (2010b). Structural implications for K5/K12-di-acetylated histone H4 recognition by the second bromodomain of BRD2. FEBS Lett. *584*, 3901–3908.

Valls, E., Sánchez-Molina, S., and Mártinez-Balbás, M.A. (2005). Role of histone modifications in marking and activating genes through mitosis. J. Biol. Chem. *280*, 42592–42600.

Viejo-Borbolla, A., Ottinger, M., Brüning, E., Bürger, A., König, R., Kati, E., Sheldon, J.A., and Schulz, T.F. (2005). Brd2/RING3 interacts with a chromatin-binding domain in the Kaposi's Sarcoma-associated herpesvirus latency-associated nuclear antigen 1 (LANA-1). J. Virol. *79*, 13618–13629.

Yang, X.-J., and Seto, E. (2007). HATs and HDACs: from structure, function and regulation to novel strategies for therapy and prevention. Oncogene *26*, 5310–5318.

Yoshida, M., and Beppu, T. (1988). Reversible arrest of proliferation of rat 3Y1 fibroblasts in both the G1 and G2 phases by trichostatin A. Exp. Cell Res. *177*, 122–131.

Yoshida, M., Kijima, M., Akita, M., and Beppu, T. (1990). Potent and specific inhibition of mammalian histone deacetylase both in vivo and in vitro by trichostatin A. J. Biol. Chem. *265*, 17174–17179.

Zeng, L., and Zhou, M.M. (2002). Bromodomain: an acetyl-lysine binding domain. FEBS Lett. *513*, 124–128.